DOI: 10.3901/CJME.2013.05.873, available online at www.springerlink.com; www.cjmenet.com; www.cjmenet.com.cn

Feedback Attitude Sliding Mode Regulation Control of Spacecraft Using Arm Motion

SHI Ye[1, *], LIANG Bin[2], XU Dong[3], WANG Xueqian[2], and XU Wenfu[4]

1 *Qian Xuesen Laboratory of Space Technology, Beijing 100094, China*
2 *Dongfanghong Development Ltd Shenzhen, Shenzhen 518057, China*
3 *Beijing Military Command Area, 66240 Troops, Beijing 100043, China*
4 *Shenzhen Graduate School, Harbin Institute of Technology, Shenzhen 518055, China*

Received August 24, 2012; revised June 13, 2013; accepted June 17, 2013

Abstract: The problem of spacecraft attitude regulation based on the reaction of arm motion has attracted extensive attentions from both engineering and academic fields. Most of the solutions of the manipulator's motion tracking problem just achieve asymptotical stabilization performance, so that these controllers cannot realize precise attitude regulation because of the existence of non-holonomic constraints. Thus, sliding mode control algorithms are adopted to stabilize the tracking error with zero transient process. Due to the switching effects of the variable structure controller, once the tracking error reaches the designed hyper-plane, it will be restricted to this plane permanently even with the existence of external disturbances. Thus, precise attitude regulation can be achieved. Furthermore, taking the non-zero initial tracking errors and chattering phenomenon into consideration, saturation functions are used to replace sign functions to smooth the control torques. The relations between the upper bounds of tracking errors and the controller parameters are derived to reveal physical characteristic of the controller. Mathematical models of free-floating space manipulator are established and simulations are conducted in the end. The results show that the spacecraft's attitude can be regulated to the position as desired by using the proposed algorithm, the steady state error is 0.000 2 rad. In addition, the joint tracking trajectory is smooth, the joint tracking errors converges to zero quickly with a satisfactory continuous joint control input. The proposed research provides a feasible solution for spacecraft attitude regulation by using arm motion, and improves the precision of the spacecraft attitude regulation.

Key words: attitude regulation, space robot, trajectory tracking, sliding mode control

1 Introduction

For the purpose of both the survival of a satellite and the satisfactory achievement of on orbit operations, spacecraft attitude must be regularly controlled. Conventionally, momentum wheel and thrusters are two typical mechanisms to fulfill this task. However, for momentum wheel, the off-loading problem needs to be considered and the use of thrusters would consume the non-renewable fuels[1–2]. Thus other attitude control methods are required as a replacement to realize the attitude control tasks.

For spacecraft equipped with additional appendages, for example manipulators, when the attitude control system of the spacecraft is closed, the angular momentum of the whole system conserves. The non-holonomy is the essential nature of the system[3–4]. So, the uncontrolled spacecraft would have a coupling movement caused by the motion of the manipulators. This makes it possible to regulate the spacecraft attitude by controlling the arm motions. Using additional appendages to perform spacecraft attitude regulation tasks is first proposed by REYHANOGLU, et al[5]. In their research, a reorientation maneuvering strategy for an interconnection of planar rigid bodies in space is developed and applied to a specific space maneuver of a three body interconnection. In the past decades, considerable research has been done in this area.

YAMADA[6] stablished the relation between the variation of the base attitude and that of the joint angles. On the basis of this relation, an algorithm for the joint angle path planning was proposed to regulate spacecraft attitude to the desired position. Further, taking the additional constraints such as joint limits of the manipulators, a surface integral approach for the motion planning of the manipulators was presented by MUKHERJEE, et al[7]. Still, the problem of reorienting the satellite was reformulated to a steering problem for a drift free control system and was solved from the perspective of control theories by WALSH, et al[8]. VAFA and DUBOWSKY[9] used cyclic motion of the space manipulator to change the satellite orientation. This scheme requires many cycles to make even a small change in vehicle orientation. On the basis of cyclic arm motion, feedback control of space robot attitude was developed by YAMADA, et al[10]. In their research the

* Corresponding author. E-mail: shiye_hit@hotmail.com
This project is supported by National Natural Science Foundation of China(Grant No. 61175098)

model errors and disturbances have been taken into consideration. Optimal control theory is developed by CERVEN, et al[11], to minimize the required control efforts in determining the arm motion. XU, et al[12] developed an trajectory planning method for base reorientation of free-floating space robotic system after capturing target. SHI, et al[13] proposed a path planning approach to realize the Cartesian pose of the end effector and the attitude of spacecraft attaining the desired states simultaneously. Quantum behaved particle swarm optimization algorithm was used to solve a nonlinear optimization problem.

Most of the above mentioned researches used to solve the reorientation problems just discussed the path planning problem. The relationship between the attitude change of the spacecraft and the manipulator motions was derived. Then it was used to determine the desired manipulator motions based on the desired spacecraft attitude. However, given the desired path of the manipulator, the precise tracking is not always possible. Disturbances caused by friction and/or actuator failures do always exist. Under this situation, the desired path generated by the path planning algorithm will not always be precisely followed. For free-floating multibody space structures, the non-holonomic property suggests that when the precise path following can't be fulfilled, the predefined attitude regulation/tracking will fail. Thus, how to control the movement of robot arms to precisely following the predefined path from the start should be extensively studied. However, most of the researches only provide path planning algorithms; few of them have discussed this tracking problem.

Sliding mode control is a control algorithm using switched control actions to prescribe the system dynamics to a predefined manifold. When the sliding manifold is reached, robustness to modeling uncertainties and external disturbances is achieved. Thus sliding mode control is widely used in control areas[14–16]. Sliding mode control has been addressed in some previous studies for spacecraft attitude control problems[17–20]. However, the control problem studied in those studies is different from which will be discussed. The general control problem of path following can be concluded to be successful if the tracking error converges to zero when time evolves to infinity. However, the control task studied in this paper requires that the tracking error stays on the zero line permanently from the beginning. Thus the existing sliding mode control laws should be reinvestigated carefully.

In this paper, the precise path following control problem is studied. Sliding mode control techniques are utilized to confine the tracking errors stay on the zero line permanently. To avoid the chattering phenomenon, saturation function is used. The relation between attitude regulation accuracy and controller parameters is deduced. In the end, simulations are conducted with the comparison of computed torque control law to show the effectiveness of the proposed controller. The paper is organized as follows: Section 2 presents the model description. Section 3 illustrates the researched problems with simulations; the control system design is presented in section 4. Simulation results of a two link free-floating space robot are presented in section 5.

2 Modeling of Space Robotic System

The dynamic model for a rigid n-link, serially connected, direct driven revolute space robot is given as follows[21]:

$$\boldsymbol{M}(\boldsymbol{q})\ddot{\boldsymbol{q}}+\boldsymbol{C}(\boldsymbol{q},\ \dot{\boldsymbol{q}})\dot{\boldsymbol{q}}=\boldsymbol{\tau}+\boldsymbol{\tau}_{\mathrm{d}}\,, \tag{1}$$

where $\boldsymbol{q}$, $\dot{\boldsymbol{q}}$, $\ddot{\boldsymbol{q}}$ —Spacecraft and manipulator joint angles, velocity and acceleration vectors,

$\boldsymbol{M}(\boldsymbol{q})$ —Robot inertial matrix,

$\boldsymbol{C}(\boldsymbol{q},\ \dot{\boldsymbol{q}})\dot{\boldsymbol{q}}$ —Centripetal coriolis force,

$\boldsymbol{\tau}$ —Control inputs torque,

$\boldsymbol{\tau}_{\mathrm{d}}$ —Bounded external disturbance.

The dynamic model Eq. (1) developed with Euler Lagrange equation possesses properties 1, 2[12].

Property 1: The positive definite and symmetric inertia matrix satisfies the following inequalities:

$$m_1\|\zeta\|^2 \leqslant \zeta^{\mathrm{T}}\boldsymbol{M}(\boldsymbol{q})\zeta \leqslant m_2\|\zeta\|^2, \quad \forall \zeta\in\mathbf{R}^n, \tag{2}$$

where $m_1, m_2 \in \mathbf{R}$ are known positive bounding constants.

Property 2: The time derivative of the inertia matrix and the centripetal Coriolis matrix satisfy the following skew symmetric relationship[22]:

$$\zeta^{\mathrm{T}}\left(\dot{\boldsymbol{M}}(\boldsymbol{q})-2\boldsymbol{C}(\boldsymbol{q},\dot{\boldsymbol{q}})\right)\zeta=0, \quad \forall\zeta\in\mathbf{R}^n. \tag{3}$$

Remark 1: The skew symmetric relationship illustrated in Property 2 indicates the passivity property of Eq. (1) with respect to input τ and output $\dot{\boldsymbol{q}}$. This means the negative feedback connection of joint velocities $\dot{\boldsymbol{q}}$ would stabilize the space manipulator system to its equilibrium manifold.

3 Problem Formulation

Simulations are conducted to illustrate the problems to be solved and the form problem definition is given subsequently. Here, a reorientation problem for the spacecraft of a two link planar space robot needs to be solved. The initial spacecraft attitude is 0 rad, and it is required to be regulated to 0.908 rad. On the basis of the path planning algorithms, one possible trajectory for manipulator joints is chosen as

$$
\begin{aligned}
q_1(t) &= (t^3 - 15t^2)/500, \\
q_2(t) &= (2t^3 - 30t^2)/500.
\end{aligned} \tag{4}
$$

When precise tracking is achieved, the spacecraft attitude will become 0.908 rad at 10 s and its velocity will be zero.

The physical parameters of this simulated space robot are listed in Table 1, where m_i and I_i are the mass and the moment of inertia of the i-th rigid body, respectively, a_i and b_i are shown in Fig. 1

Table 1. Physical Parameters of the Space Robot

Body	Link length		Body mass	Body inertia
	a_i/m	b_i/m	m_i/kg	I_i/(kg • m^2)
Base	—	0.5	4	0.4
Link 1	0.5	0.5	1	0.1
Link 2	0.5	0.5	1	0.1

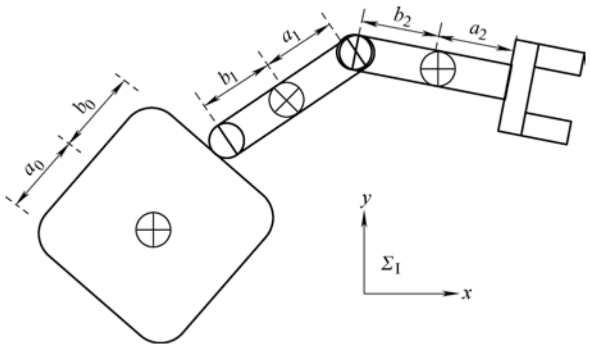

Fig. 1 Configuration of the simulation model

In the simulation, the system states are initialized to be zero. Then the simulation is conducted with the computed torque control law[23] ,which gives the form of

$$\boldsymbol{\tau}_{\mathrm{m}} = \boldsymbol{B}(\ddot{\boldsymbol{q}}_{\mathrm{md}} - k_{\mathrm{d}}\dot{\boldsymbol{e}} - k_{\mathrm{p}}\dot{\boldsymbol{e}}) + \boldsymbol{V}(\boldsymbol{q}_{\mathrm{m}},\ \dot{\boldsymbol{q}})\dot{\boldsymbol{q}}_{\mathrm{m}},$$

where $k_{\mathrm{d}} = 3, k_{\mathrm{p}} = 2$ and $\boldsymbol{B}$, $\tilde{\boldsymbol{V}}$, $\boldsymbol{e}$, $\boldsymbol{s}$, $\boldsymbol{f}$ are defined in section 4.

With the assumption of exact knowledge of system dynamics and no external disturbance, the simulation results are shown in Fig. 2.

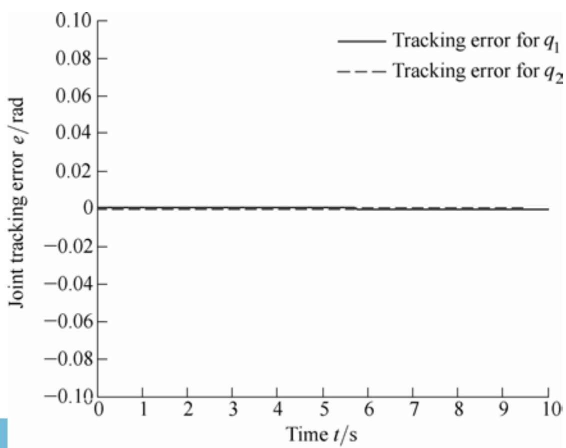

(a) Manipulator joint space tracking errors

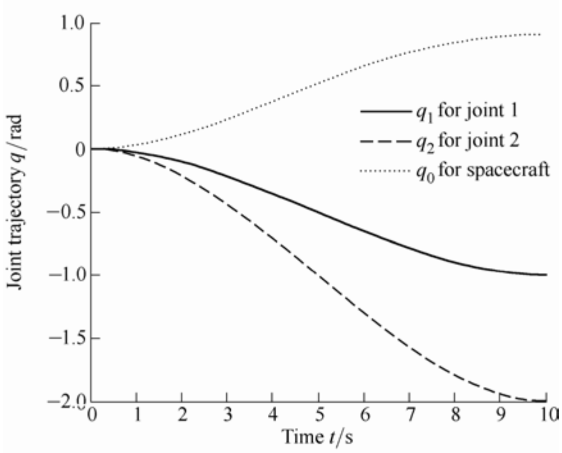

(b) Tracking trajectories of spacecraft and manipulator joints

Fig. 2 Simulated results with no disturbances

From the simulation results, it can be observed that the spacecraft attitude will become 0.908 rad after 10 s. When there exists external disturbance, for example the following impulse disturbance at 1 s,

$$\boldsymbol{d}(t) = \begin{cases} 10, & 1 < t < 2, \\ 0, & \text{others}. \end{cases} \tag{5}$$

The computed torque control would appear a period of deviation, see Fig. 3.

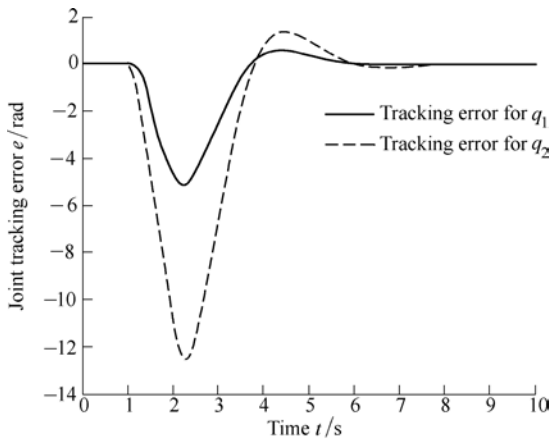

(a) Manipulator joint space tracking errors

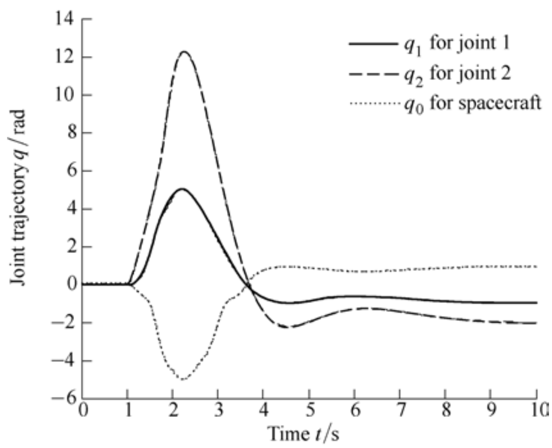

(b) Tracking trajectories of spacecraft and manipulator joints

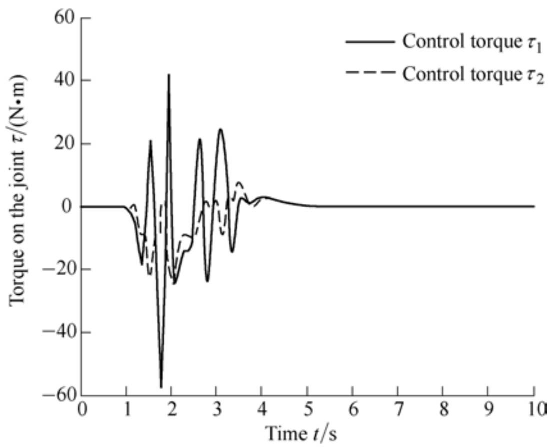

(c) Control torque applied on the manipulator joints

Fig. 3　Simulated results with external disturbance

It can be observed that in spite of the disturbance, the manipulator joint tracking error quickly converges to zero which means the closed loop system is still stable. However, at the end of simulation, the spacecraft attitude becomes to be 0.945 1 rad. This is caused by the non-holonomic structure of the free-floating space robots. The attitude change of the spacecraft is not just decided by the initial and ending position of the manipulator joints. Actually, it is a function of the entire trajectory of manipulator joints. Thus, if the precise following is not achieved, the actual spacecraft attitude would deviate from the desired one at the end of the task.

From this perspective of view, the control object required in this task is to command the motion of manipulator joints to precisely tracking the given planned path to make the tracking error equals to zero permanently, i.e. $\boldsymbol{e}\equiv 0$.

4　Feedback Sliding Mode Attitude Regulation Control

Sliding mode control techniques use the sign function to realize the switched control effects. The introduction of switched control effects would enforce the system trajectory to stay on the sliding manifold even in the presence of disturbances. In the following, sliding mode control law is designed to realize the control objects.

4.1　Sliding mode control with sign functions

The manipulator dynamics in Eq. (1) can be partitioned as

$$\boldsymbol{m}_{11}\ddot{\boldsymbol{q}}_{\rm b}+\boldsymbol{m}_{12}\ddot{\boldsymbol{q}}_{\rm m}+\boldsymbol{h}_1=\tau_{\rm ds}\,, \tag{6}$$

$$\boldsymbol{m}_{21}\ddot{\boldsymbol{q}}_{\rm b}+\boldsymbol{m}_{22}\ddot{\boldsymbol{q}}_{\rm m}+\boldsymbol{h}_2=\boldsymbol{\tau}_{\rm m}+\tau_{\rm dm}\,, \tag{7}$$

where $\boldsymbol{q}_{\rm b}$, $\boldsymbol{q}_{\rm m}$ represent the generalized coordinates for spacecraft and manipulator respectively and $\boldsymbol{h}_1=\boldsymbol{c}_{11}\dot{\boldsymbol{q}}_{\rm b}+\boldsymbol{c}_{12}\dot{\boldsymbol{q}}_{\rm m},\boldsymbol{h}_2=\boldsymbol{c}_{21}\dot{\boldsymbol{q}}_{\rm b}+\boldsymbol{c}_{22}\dot{\boldsymbol{q}}_{\rm m}$. If $\ddot{\boldsymbol{q}}_{\rm b}$ is solved from Eq. (6), Eq. (8) can be obtained:

$$\ddot{\boldsymbol{q}}_{\rm b}=\boldsymbol{m}_{11}{}^{-1}\boldsymbol{\tau}_{\rm ds}-\boldsymbol{m}_{11}{}^{-1}(\boldsymbol{m}_{12}\ddot{\boldsymbol{q}}_{\rm m}+\boldsymbol{h}_1)\,. \tag{8}$$

If Eq. (8) is substituted into Eq. (7), the following can be obtained:

$$\begin{gathered}\underbrace{(\boldsymbol{m}_{22}-\boldsymbol{m}_{21}\boldsymbol{m}_{11}^{-1}\boldsymbol{m}_{12})}_{\boldsymbol{B}(\boldsymbol{q}_{\rm m})}\ddot{\boldsymbol{q}}_{\rm m}+\underbrace{\boldsymbol{h}_2-\boldsymbol{m}_{21}\boldsymbol{m}_{11}^{-1}\boldsymbol{h}_1}_{\boldsymbol{V}(\boldsymbol{q}_{\rm m},\dot{\boldsymbol{q}})\dot{\boldsymbol{q}}_{\rm m}}=\\ \tau_{\rm m}+\underbrace{(-\tau_{\rm dm}-\boldsymbol{m}_{21}\boldsymbol{m}_{11}^{-1}\tau_{\rm ds})}_{\boldsymbol{d}},\end{gathered} \tag{9}$$

where $\boldsymbol{B}(\boldsymbol{q}_m)$ can be regarded as the transformed inertia matrix for joint variables.

$\boldsymbol{q}_m$ and $\boldsymbol{d}$ is the lumped disturbance term which is upper bounded by α, i.e. $\|\boldsymbol{d}\|\leqslant\alpha$ with norm $\|\ \|$ defined as $\|\boldsymbol{x}\|=\max_{1\leqslant i\leqslant n}|x_i|$ for n-dimensional vectors $\boldsymbol{x}$.

From the symmetric and positive definite property of inertia matrix $\boldsymbol{M}(\boldsymbol{q})$, matrix $\boldsymbol{B}(\boldsymbol{q}_{\rm m})$ is also positive definite and symmetric.

In virtual of controller design, matrix $\boldsymbol{V}$ is decomposed to $\boldsymbol{V}=\tilde{\boldsymbol{V}}+\hat{\boldsymbol{V}}$ such that $\dot{\boldsymbol{B}}-2\tilde{\boldsymbol{V}}$ is skew symmetric, i.e.

$$\boldsymbol{\zeta}^{\rm T}(\dot{\boldsymbol{B}}(\boldsymbol{q}_{\rm m})-2\tilde{\boldsymbol{V}}(\boldsymbol{q}_{\rm m},\dot{\boldsymbol{q}}))\boldsymbol{\zeta}=0\quad\forall\boldsymbol{\zeta}\in\mathbf{R}^n\,. \tag{10}$$

The following error variables and sliding vectors are defined in virtual of the synthesis of the controller:

$$\boldsymbol{e}=\boldsymbol{q}_{\rm m}-\boldsymbol{q}_{\rm md},\ \boldsymbol{s}=\dot{\boldsymbol{e}}+\boldsymbol{\lambda}\boldsymbol{e}\,, \tag{11}$$

where $\boldsymbol{\lambda}={\rm diag}[\lambda_i]>\boldsymbol{0}$. With some manipulations, Eq. (1) can be transformed to

$$\begin{gathered}\boldsymbol{B}(\boldsymbol{q}_{\rm m})\dot{\boldsymbol{s}}+\tilde{\boldsymbol{V}}(\boldsymbol{q}_{\rm m},\dot{\boldsymbol{q}})\boldsymbol{s}=\boldsymbol{\tau}_{\rm m}+\boldsymbol{f}(\boldsymbol{q}_{\rm m},\dot{\boldsymbol{q}},\boldsymbol{q}_{\rm d},\dot{\boldsymbol{q}}_{\rm d},\ddot{\boldsymbol{q}}_{\rm d})+\boldsymbol{d},\\ \boldsymbol{f}(\boldsymbol{q}_{\rm m},\dot{\boldsymbol{q}},\boldsymbol{q}_{\rm d},\dot{\boldsymbol{q}}_{\rm d},\ddot{\boldsymbol{q}}_{\rm d})=-\boldsymbol{B}\ddot{\boldsymbol{q}}_{\rm mr}-\boldsymbol{V}\dot{\boldsymbol{q}}_{\rm mr}-\hat{\boldsymbol{V}}\boldsymbol{s},\\ \dot{\boldsymbol{q}}_{\rm mr}=\dot{\boldsymbol{q}}_{\rm d}-\boldsymbol{\lambda}\boldsymbol{e}.\end{gathered} \tag{12}$$

To this end, the control law is designed as

$$\tau_{\rm m}=-\boldsymbol{f}(\boldsymbol{q}_{\rm m},\ \dot{\boldsymbol{q}},\ \boldsymbol{q}_{\rm d},\ \dot{\boldsymbol{q}}_{\rm d},\ \ddot{\boldsymbol{q}}_{\rm d})-k\,{\rm sgn}(\boldsymbol{s})\,. \tag{13}$$

Theorem 1: Given the space manipulator dynamics described by Eq. (1) in the presence of disturbances under the control law Eq. (13), the following results holds for the closed-loop system:

(i) $\boldsymbol{e},\dot{\boldsymbol{e}}$ will always equal to zero;

(ii) Control torques $\boldsymbol{\tau}_{\rm m}$ is bounded for all $t\geqslant 0$.

Proof(i): The closed-loop dynamics for space manipulators under the designed control law Eq. (13) is

$$\boldsymbol{B}\dot{\boldsymbol{s}}+\tilde{\boldsymbol{V}}\boldsymbol{s}=-k\,{\rm sgn}(\boldsymbol{s})-\boldsymbol{d}\,. \tag{14}$$

Given the following Lyapunov function candidate

$$L_1 = \frac{1}{2} \boldsymbol{s}^{\mathrm{T}} \boldsymbol{B} \boldsymbol{s}, \tag{15}$$

the derivative of Eq. (15) along the trajectory of Eq. (14) gives

$$\dot{L}_1 \leqslant \boldsymbol{s}^{\mathrm{T}}(-k\,\mathrm{sgn}(\boldsymbol{s})) + \|\boldsymbol{s}\|\|\boldsymbol{D}\| \leqslant \\ -k\|\boldsymbol{s}\| + \alpha\|\boldsymbol{s}\| \leqslant -\|\boldsymbol{s}\|(k-\alpha). \tag{16}$$

Because the inequality $\boldsymbol{s}^{\mathrm{T}}\boldsymbol{B}\boldsymbol{s} \leqslant \|\boldsymbol{s}\|^2 \lambda_{\max}(\boldsymbol{B})$ holds, from Eq. (15), $\|\boldsymbol{s}\|$ is lower bounded by

$$\|\boldsymbol{s}\| \geqslant \sqrt{\frac{2L_1}{\lambda_{\max}(\boldsymbol{B})}}. \tag{17}$$

Thus, combining Eq. (16) one get

$$\dot{L}_1 \leqslant -(k-\alpha)\sqrt{\frac{2L_1}{\lambda_{\max}(\boldsymbol{B})}}. \tag{18}$$

Integrating both sides from 0 to t_{r} of the upper inequality, one get

$$2\sqrt{L_1(t_{\mathrm{r}})} - 2\sqrt{L_1(0)} \leqslant -(k-\alpha)\sqrt{\frac{2}{\lambda_{\max}(\boldsymbol{B})}}t_{\mathrm{r}}. \tag{19}$$

When the sliding surface is reached, $\boldsymbol{s}(t_r)=0$, therefore, $L_1(t_{\mathrm{r}})=0$. From Eq. (19), the reaching time is upper bounded by

$$t_{\mathrm{r}} \leqslant \sqrt{\frac{2L_1(0)\lambda_{\max}(\boldsymbol{B})}{(k-\alpha)}}. \tag{20}$$

Because $\boldsymbol{q}_{\mathrm{d}}$ is planned with the constraints $\boldsymbol{q}_{\mathrm{d}}(0)=\boldsymbol{q}(0),\ \dot{\boldsymbol{q}}_{\mathrm{d}}(0)=\dot{\boldsymbol{q}}(0)$, thus $\boldsymbol{e}(0)=0,\ \dot{\boldsymbol{e}}(0)=0,$ which means $\boldsymbol{s}(0)=0.$ Further we can conclude that $L_1(0)=0$, so Eq. (20) turns to be

$$t_{\mathrm{r}} \leqslant 0. \tag{21}$$

Then, we know that $t_{\mathrm{r}}=0$, so the sliding surface is reached at the beginning. Solving the ordinary differential equation $\dot{\boldsymbol{e}}+\boldsymbol{\lambda}\boldsymbol{e}=0$ with zero initial values, $\boldsymbol{e}$ and $\dot{\boldsymbol{e}}$ always equal zero even with the existences of bounded disturbances.

Proof(ii): From the boundness of reference path $\boldsymbol{q}_{\mathrm{d}}$, the boundness of $\boldsymbol{q}$ and sliding vector $\boldsymbol{s}$ can be established, and furthermore we can conclude that the torques generated by control law Eq. (13) is also bounded.

Remark 2: The construction of skew symmetric relations in Eq. (10) is to render the transformed system Eq. (12) to be passive with respect to input $\boldsymbol{\tau}$ and output $\boldsymbol{s}$. Thus the designed negative feedback connection of $\boldsymbol{s}$ (in the form of sign($\boldsymbol{s}$) in Eq. (13)) would stabilize the sliding vector $\boldsymbol{s}$ to zero. Because $\boldsymbol{s}$ is a stable manifold, once the system trajectory reaches $\boldsymbol{s}$, the tracking error dynamics would naturally evolve to the stable equilibrium. Thus, the trajectory tracking purpose would be achieved. This is the physical interpretation of the designed sliding mode control law.

4.2 Sliding mode control with saturation functions

For the designed control law Eq. (13), the introduction of sign function would inevitably result in the chattering phenomenon. In this part, the saturation strategy is used to eliminate the chattering phenomenon. The new controller is modified to

$$\boldsymbol{\tau}_{\mathrm{m}} = \begin{cases} -\boldsymbol{f}(\boldsymbol{q}_{\mathrm{m}},\dot{\boldsymbol{q}},\boldsymbol{q}_{\mathrm{d}},\dot{\boldsymbol{q}}_{\mathrm{d}},\ddot{\boldsymbol{q}}_{\mathrm{d}}) - k_1\,\mathrm{sgn}(\boldsymbol{s}), & \|\boldsymbol{s}\| > \epsilon, \\ -\boldsymbol{f}(\boldsymbol{q}_{\mathrm{m}},\dot{\boldsymbol{q}},\boldsymbol{q}_{\mathrm{d}},\dot{\boldsymbol{q}}_{\mathrm{d}},\ddot{\boldsymbol{q}}_{\mathrm{d}}) - k_2\dfrac{\boldsymbol{s}}{\delta}, & \|\boldsymbol{s}\| \leqslant \epsilon, \end{cases} \tag{22}$$

where ϵ is a small value. k_1, k_2, δ are positive control gains, which satisfy $\delta\alpha/k_2 < \epsilon$.

Theorem 2: Consider the space manipulator dynamics described by Eq. (1) in the presence disturbances under the control law Eq. (22), the following result holds for the closed-loop system.

(a) The tracking error is upper bounded by $\delta\alpha/\lambda k_2$, i.e. $\|e(t)\| \leqslant \delta\alpha/\lambda k2$.

(b) The control torque $\boldsymbol{\tau}_m$ is bounded for all $t \geqslant 0$.

Proof (a): The new Lyapunov function is defined to be

$$L_2 = \frac{1}{2}\boldsymbol{s}^{\mathrm{T}}\boldsymbol{B}\boldsymbol{s}. \tag{23}$$

Then the derivatives of the defined Lyapunov function along the system dynamics gives to be

$$\dot{L}_2 \leqslant \boldsymbol{s}^{\mathrm{T}}(\boldsymbol{\tau}_{\mathrm{m}} + \boldsymbol{f}(\boldsymbol{q}_{\mathrm{m}},\dot{\boldsymbol{q}},\boldsymbol{q}_{\mathrm{d}},\dot{\boldsymbol{q}}_{\mathrm{d}},\ddot{\boldsymbol{q}}_{\mathrm{d}})) + \|\boldsymbol{s}\|\alpha. \tag{24}$$

When $\boldsymbol{s}(0)=0$, according to Eq. (22), the control torque applied should be $\tau_m = 0 - \boldsymbol{f}(\boldsymbol{q}_m,\dot{\boldsymbol{q}},\boldsymbol{q}_d,\dot{\boldsymbol{q}}_d,\ddot{\boldsymbol{q}}_d) - k_2\dfrac{\boldsymbol{s}}{\delta}$. During a small time period after 0, Eq. (25) can be obtained:

$$\dot{L}_2 \leqslant -k_2\frac{\|\boldsymbol{s}\|^2}{\delta} + \|\boldsymbol{s}\|\alpha = -\|\boldsymbol{s}\|\left(\frac{k_2}{\delta}\|\boldsymbol{s}\| - \alpha\right). \tag{25}$$

Because $s(0)=0$, the predefined Lyapunov function will increase until

$$\dot{L}_2 < 0, \tag{26}$$

which requires

$$\|s\| > \frac{\delta\alpha}{k_2}. \tag{27}$$

Because $\delta\alpha/\lambda k_2$ is less than $\in$, when s goes beyond this constraint, $\dot{L}_2$ will turn to be negative. The control input will confine the sliding vector s goes back and stays into the boundary layer $\delta\alpha/k_2$. Thus, eventually, the sliding vector will be upper bounded by

$$\|s\| > \frac{\delta\alpha}{k_2}. \tag{28}$$

From the definition $\dot{\boldsymbol{e}}+\boldsymbol{\lambda e}=\boldsymbol{s}$, the solution for the ordinary differential equation is

$$\boldsymbol{e}(t)=\exp(-\lambda t)\boldsymbol{e}(0)+\exp(-\lambda t)\int_0^1 \exp(\lambda t)\boldsymbol{s}\mathrm{d}t. \tag{29}$$

Then

$$\|\boldsymbol{e}(t)\| \leqslant \exp(-\boldsymbol{\lambda} t)\boldsymbol{e}(0)+\exp(-\boldsymbol{\lambda} t)\|\boldsymbol{s}\|\int_0^t \exp(\boldsymbol{\lambda} t)\,\mathrm{d}t \leqslant$$
$$\exp(-\boldsymbol{\lambda} t)\boldsymbol{e}(0)+\|\boldsymbol{s}\|\frac{1-\exp(-\boldsymbol{\lambda} t)}{\boldsymbol{\lambda}}. \tag{30}$$

Because $\boldsymbol{e}(0)=0$, the tracking error is upper bounded by

$$\|e(t)\| \leqslant \frac{\|\boldsymbol{s}\|}{\lambda}=\frac{\delta\alpha}{\lambda k_2}. \tag{31}$$

Proof (b): From the boundness of reference path $\boldsymbol{q}_{\mathrm{d}}$, the boundness of $\boldsymbol{q}$ and sliding vector $\boldsymbol{s}$ can be established, and the further we can conclude that the control torque generated by Eq. (22) is also bounded.

Remark 3: In Theorem 2, uniformly ultimately boundness property of the tracking error can be established. The tracking error can be made arbitrary small by tuning the control parameters. Thus the required attitude reorientation accuracy can always be achieve by properly choosing values for $\lambda, k_1, k_2, \delta$.

5 Simulation

To demonstrate the effectiveness of the proposed control schemes, numerical simulations are performed and presented in this section. The form of disturbances is the same to the one used in section 3, and the control object is also the same to the simulations conducted in Section 3, i.e. to regulate the spacecraft attitude from 0 rad to 0.908 rad. The reference path for manipulator joints is also the same one, that is

$$\begin{aligned} q_1(t)&=(t^3-15t^2)/500, \\ q_2(t)&=(2t^3-30t^2)/500. \end{aligned} \tag{32}$$

Both conventional sliding mode control with sign function and improved saturation sliding mode control are simulated. The simulation results are shown in the following figures. Figs. 4–5 show the simulated results using sliding mode control with sign functions in which the control parameter is set to be $\lambda=2,\ k=25$. The tracking errors and trajectories are shown in Fig. 4, the dynamics of the sliding surface and torques response are given in Fig. 5.

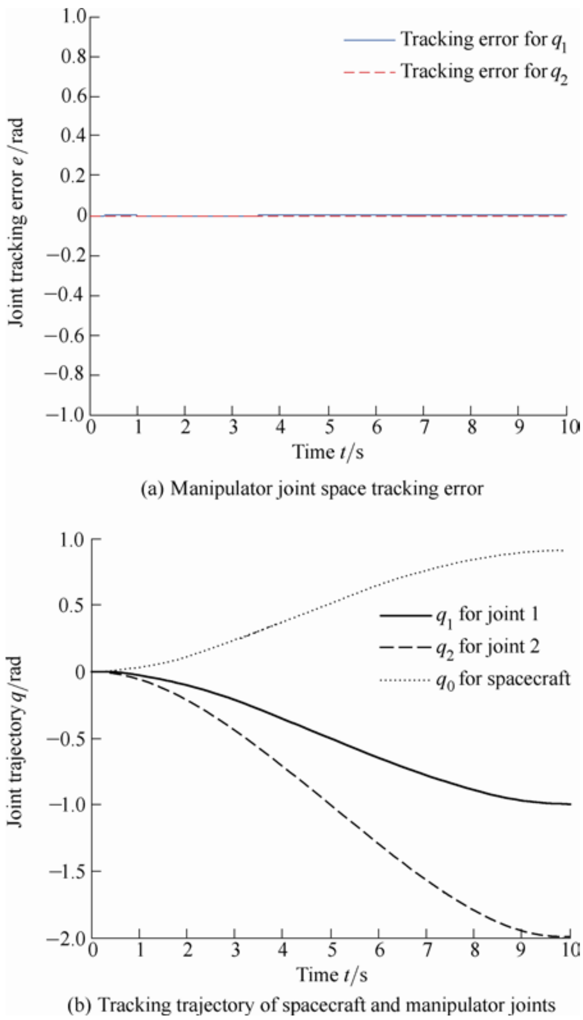

(b) Tracking trajectory of spacecraft and manipulator joints

Fig. 4 Sliding mode control with disturbance

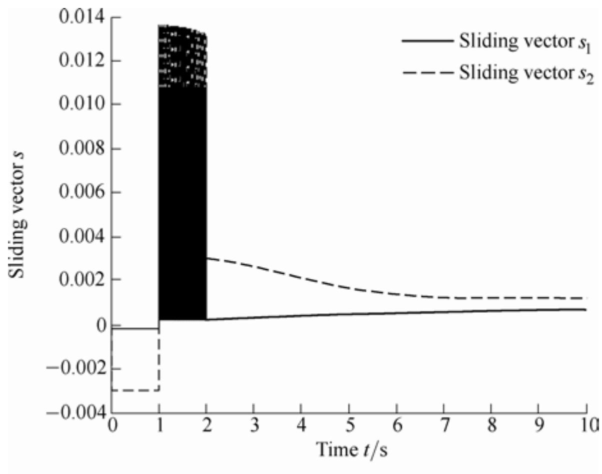

(a) Dynamics of the sliding vector

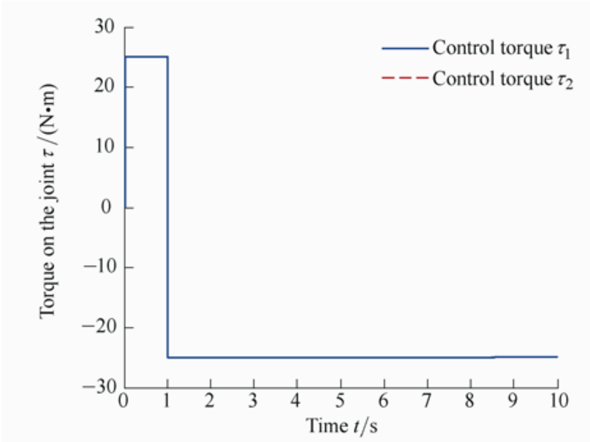

(b) Control torque acting on the manipulator joints

Fig. 5 Sliding mode control with disturbance

The simulation results show that the actual manipulator joint precisely tracks the given ones. In spite of the disturbance torque, an acceptable desirable orientation response is achieved, and the spacecraft reaches the demanded angle with a settling time 10 s. Moreover, the amplitude of control torque is not more than the 25 N • m. But, it can be observed from Fig.5 (a) that the introduction of the sign function generates the chattering phenomenon.

Fig. 6 and Fig. 7 show simulation results with sliding mode control with saturation functions. In order to guarantee system convergence and achieve robustness, the control parameters are set to be $\lambda=2$, $\epsilon=0.5$, $k_1=25$, $k_2=5$ and $\delta=0.01$. The tracking errors and trajectories are shown in Fig. 6; the dynamics of the sliding surface and torques response are given in Fig. 7.

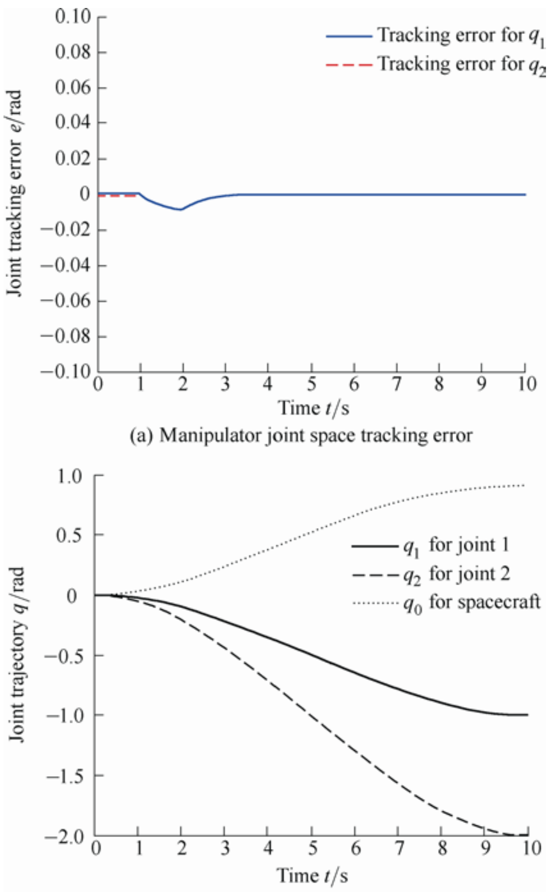

(b) Tracking trajectory of spacecraft and manipulator joints

Fig. 6 Saturation sliding mode control with disturbance

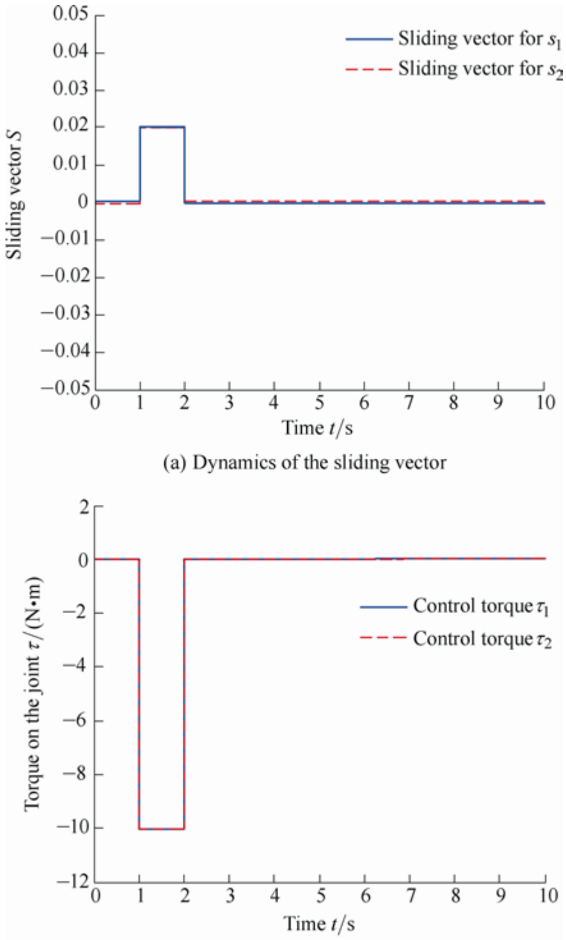

(b) Control torque acting on the manipulator joints

Fig. 7 Saturation sliding mode control with disturbance

From Fig. 7 it can be observed that the chattering phenomenon is eliminated. However, this is achieved at the price of a bounded sliding vector. Further, the tracking error can only be bounded by 0.01 from Fig. 6(a). But this does not affect the spacecraft reorientation accuracy. At the end of the simulation, the spacecraft attitude is regulated to 0.907 8 rad shown in Fig. 6(b).

Extensive simulations are also done with different disturbance inputs. The results show that the proposed approach is feasible to regulate spacecraft attitude in spite of disturbance existence. Moreover, the flexibility in the choice of control parameters can be utilized to obtain the desirable performance.

6 Conclusions

(1) An approach based on variable structure control is presented, and the relation between the upper bounds of the tracking errors and the controller parameter is derived. This approach can realize precise attitude regulation of the spacecraft by using arm motion.

(2) The non-zero initial tracking errors and chattering phenomenon can be solved through replacing the sign functions by saturation functions.

(3) The proposed control system is proved stable based on Lyapunov theory. The simulation results indicate that the proposed control approach is effective, and its performance is better than that of computed torque control law.

References

[1] WAYER J K, CASTET J F, SALEH J H. Spacecraft attitude control subsystem: reliability, multi-state analyses and comparative failure behavior in LEO and GEO[J]. *Acta Astronautica*, 2013, 85(3): 83–92.

[2] FAN J X, ZHOU D. Nonlinear attitude control of spacecraft based on scissor pairs of control moment gyroscope[J]. *Journal of Mechanical Engineering*, 2010, 46(8): 154–159.

[3] MATSUMOTO S, WAKABAYASHI Y, WATANABE Y. Attitude control for free-flying space robot using gravity gradient torque and manipulator posture[C]//*AIAA Guidance and Control Conference, Denver*, CO, August 14–17, 2000: 34–40.

[4] XU W F, LIANG B. Survey of modeling, planning, and ground verification of space robotic systems[J]. *Acta Astronautica*, 2011, 68: 1 629–1 649.

[5] REYHANOGLU M, MCCLAMROCH N H. Planar reorientation maneuvers of space multibody systems using internal controls[J]. *Journal of Guidance Control and Dynamics*, 1992, 15(6): 1 475–1 480.

[6] YAMADA K. Attitude control of space robot by arm motion[J]. *Journal of Guidance Control and Dynamics*, 1994, 17(5): 1 050–1 054.

[7] MUKHERJEE R, ZUROWSKI M. Reorientation of a structure in space using a 3-link rigid manipulator[J]. *Journal of Guidance Control and Dynamics*, 1994, 17(4): 840–847.

[8] WALSH G C, SASTRY S S. On reorienting linked rigid bodies using internal motions[J]. *IEEE Transactions on Robotics and Automation*, 1995, 11(1): 139–146.

[9] VAFA Z, DUBOWSKY S. On the dynamics of space manipulator using the virtual manipulator with application to path planning[J]. *Journal of the Astronautical Science*, 1990, 38(4): 441–472.

[10] YAMADA K, YOSHIKAWA S. Feedback control of space robot attitude by cyclic arm motion[J]. *Journal of Guidance* Control *and Dynamics*, 1997, 20(4): 715–720.

[11] CERVEN W T, COVERSTONE V L. Optimal reorientation of a multibody spacecraft through joint motion using averaging theory[J]. *Journal of Guidance Control and Dynamics,* 2001, 24(4): 788–795.

[12] XU W F, LI C, LIANG B, et al. Target berthing and base reorientation of free-floating space robotic system after capturing[J]. *Acta Astronautica*, 2009, 64(2–3): 109–126.

[13] SHI Ye, LIANG Bin, et al. Cartesian non-holonomic path planning of space robot based on quantum behaved particle swarm optimization algorithm[J]. *Chinese Journal of Mechanical Engineering*, 2011, 17(47): 99–107. (in Chinese)

[14] DECARLO R A, ZAK S H, MATTHEWS G P. Variable structure control of nonlinear multivariable systems: a tutorial[J]. *Proceedings of the IEEE*, 1988, 76(3): 212–232.

[15] GAO W B, HUNG J C. Variable structure control of nonlinear-systems: a new approach[J]. *IEEE Transactions on Industrial Electronics*, 1993, 40(1): 45–55.

[16] YOUNG K D, UTKIN V I, OZGUNER U. A control engineer's guide to sliding mode control[J]. *IEEE Transactions on Control Systems Technology*, 1999, 7(3): 328–342.

[17] CHEN Z, CHEN L. Fuzzy adaptive control for grasped objects by closed cahin space manipulator based on integral sliding mode[J]. *Acta Aeronautica et Astronautica Sinica*, 2010, 31(12): 2 442–2 449.

[18] REN Y Q, MA B L. adaptive control of space robot system based on back stepping Design[J]. *Acta Aeronautica et Astronautica Sinica*, 2007, 28(2): 490–494.

[19] CHEN Y P, LO S C. Sliding-mode controller design for spacecraft attitude tracking maneuvers[J]. *IEEE Transactions on Aerospace and Electronic Systems*, 1993, 29(4): 1 328–1 333.

[20] XUE L J, HU S H, QIANG W Y, et al. Distributed control of space robot based on sliding mode control[J]. *Control Engineering of China*, 2009, 2(16): 5–10.

[21] TIAN Zhixiang, WU Hongtao. Spatial operator algebra for free-Floating space robot modeling and simulation[J]. *Chinese Journal of Mechanical Engineering*, 2010, 23(2): 635–640.

[22] DING X L, ZHAN Q, XIE Y W. Dynamic Singularity analysis and motion planning of free-floating space robot systems[J]. *Acta Aeronautica et Astronautica Sinica*, 2001, 22(5): 474–77.

[23] AN C H, ATKESON C G, GRIFFITHS J D, et al. Experimental evaluation of feedforward and computed torque control[J] *IEEE Transactions on Robotics and Automation*, 1989, 5(3): 368–373.

Biographical notes

SHI Ye, born in 1981, is currently an engineer at *Qian Xueshen Laboratory of Space Technology*, *China*. His research interests include dynamics and control of space robotic systems, optimal path planning and control for non-holonomic system, robust adaptive control and visual servo.
Tel: +86-10-18618267148; E-mail: shiye_hit@hotmail.com

LIANG Bin, born in 1968, is currently a professor at *Department of Control Science and Engineering, Harbin Institute of Technology*, *China*. His research interests include on-orbit service, control of robotic mechanisms.
E-mail: bliang@robotsat.com

XU Dong, born in 1988, is currently an engineer at *Beijing Military Command Area, 66240 Troops*. His research interests include teleoperation of space robot.
E-mail: hce56xed@163.com

WANG Xueqian, born in 1980, is currently a post-doctor at *Department of Control Science and Engineering, Harbin Institute of Technology, China*. His research interests include space robot parameters identification.
E-mail: xqwang@robotsat.com

XU Wenfu, is currently an associate professor at *Shenzhen Graduate School, Harbin Institute of Technology*, *China.* His main research interests include space robot, modeling and intelligent control of complex system.
E-mail: wfxu@robotsat.com